Available online at www.sciencedirect.com

ScienceDirect

Energy Procedia 137 (2017) 514–522

Energy Procedia

www.elsevier.com/locate/procedia

14th Deep Sea Offshore Wind R&D Conference, EERA DeepWind'2017, 18-20 January 2017, Trondheim, Norway

Mesh Parametric Study for Fatigue Assessment of Tubular K-joints using Numerical Methods

Jorge Mendoza Espinosa[a,b,*], Sebastian Schafhirt[b], Michael Muskulus[b]

[a]*Department of Civil and Environmental Engineering, Norwegian University of Science and Technology. Trondheim 7491, Norway.*
[b]*Ramboll Wind. Hamburg 20097, Germany.*

Abstract

Wind turbine jacket structures are complex structures, whose joints design is generally driven by fatigue. These joints, along with their complex welds, are of special interest in terms of cost reduction. Therefore, a thorough analysis and understanding of the background behind the assessment proposed in guidelines is motivated. The paper presents a study of the influence of meshing for the assessment of tubular K-joints following the hot-spot approach using numerical methods. The accuracy of the results is discussed for several mesh layouts. The influence of the mesh density, element shape and element type are investigated. Furthermore, a parametric study is performed in order to see the variation of the results for several diameters, thicknesses and brace inclination combinations. The hot-spot method is proved to be robust regarding mesh regularity. However, the efficiency of irregular mesh models is very low and a high number of elements is needed in order to find an asymptotic behaviour that tends to a constant solution for increasing mesh refinement. Conclusions can be drawn for which cases it is worth to invest time in semi-automatic meshing. A discussion is done regarding which element size and type is better regarding accuracy and computational time.

Peer-review under responsibility of SINTEF Energi AS.

Keywords: Offshore; Jacket; K-joint; hot-spot; FEM; mesh

1. Introduction

Jacket support structures are a preferred solution for Offshore Wind Turbines (OWT) in deeper waters. The lattice structure has advantages over other types of support structures, such as high strength to weight ratio and the inherent property of the tubular members minimizing hydrodynamic forces. Extensive knowledge exists in relation to its construction technique as well as its crucial components, but due to considerable cost pressure, continued optimization is essential for future competitiveness of jacket structures as a support structure for OWT. A significant share of the overall production costs of jacket structures is related to the joints connecting the tubular members. Hence, these joints along with their complex welds are of special interest in terms of cost reduction.

* Corresponding author. Tel.: +34-617-142-119.
E-mail address: jorgemendozaesp@gmail.com

1876-6102 © 2017 The Authors. Published by Elsevier Ltd.
Peer-review under responsibility of SINTEF Energi AS.
10.1016/j.egypro.2017.10.380

The design of tubular joints is generally driven by fatigue resistance. The hot-spot method, as described in standards such as DNV-GL [1] or IIW [2] is commonly used in practice. Parametric formulae have been developed by several authors for the most common joint types [3,4]. Efthymiou equations [3] have been widely used due to the adoption in standards like DNV-GL [1]. His formulation introduced the influence function concept, taking care of the carry-over effect, i.e. the influence in the Stress Concentration Factor (SCF) at a reference brace due to loading in another member of the joint. However, results are quite conservative in general terms and poorly correlated to the FEM results at some cases [5]. Structural stress is found as a linear superposition of axial, in-plane and out-of-plane actions. The hot-spot stress is the maximum of structural stresses evaluated at at least eight positions around the weld. Despite this, it is demonstrated that, under different basic load combinations, the maximum peak can be found at any position along the intersection [6]. This may yield underconservative results, i.e. higher SCF can be found if evaluating the results at more than eight positions around the weld [7].

The fatigue damage of steel tubular joints is proportional to ΔS^3, given by the recommended Wöhler exponent $m = 3$ tabulated in guidelines. This means that an uncertainty of 20% on the SCF yields approximately a 70% uncertainty in fatigue life. The size, complexity, and cost of these joints lead engineers to perform analyses with detailed FEM models in order to assess their fatigue resistance.

FEM models require the definition of a mesh of discrete elements and nodes where continuum mechanics equations are to be evaluated. Different features of a mesh have to be correctly selected in order to obtain solutions with the desired accuracy. Standards suggest the use of relatively coarse regular meshes for the hot-spot stress method, with an element size in the order of the members wall thicknesses. However, these meshes are not automatically generated by commercial softwares and therefore, in engineering general practice, fine irregular meshes generated by black-box algorithms are a preferred solution. This yields higher computational time but not necessarily better results. Stress evaluation close to the weld toe is affected by the element size and type [8].

The present study was performed in order to investigate the use of automatically generated fine irregular meshes. Various meshes for several K-joint geometries were defined in the commercial software ANSYS© in order to assess their impact on the accuracy of the solution. Geometries of the simulated cases were defined for varying chord and braces diameters, thicknesses and relative angle. It should be noted that K-joints are the most common joint type in jacket support structures for OWT, but not the only one present. The analysis in this work will focus exclusively on them. It is assumed that conclusions drawn for K-joints can be extrapolated to X- and Y-joints. Further analysis should follow to validate that assumption.

Results show that automatically generated irregular fine meshes yield high computational times and for some types and positions generate significant errors. The study shows both quantitative and qualitative ideas of the relevance of meshing when performing FEM analysis in fatigue assessment using the hot-spot method. The different conceptual meshes defined were categorized regarding accuracy and computational time.

2. Description of the mathematical model

The parametric analysis of the influence of meshing in the computation of hot-spot stresses is done for three features that are assumed to be most relevant: (1) Number of elements; (2) Regularity of the mesh (and thereby the shape of the elements); (3) Element type. Furthermore, influence of the geometry of the joint is studied by varying the non-dimensional parameters defined in Fig. 1.(a) within the ranges given in Eq. (1). First of all, the FEM model is described in Section 2.1. Afterwards, in Section 2.2, the scope of the parametric investigation is defined.

The SCF is computed as the ratio between the hot-spot stress (HSS) and the nominal stress σ_n, i.e. SCF = $\frac{\text{HSS}}{\sigma_n}$. The nominal stress is defined as the stress at the same cross-section point where the hot-spot stress is evaluated, obtained by using general theories such as beam or plate theories, i.e. disregarding the peak due to local geometry. Far from the joint influence, the SCF is equal to one. The hot-spot stress is computed, according to DNV-GL [1], as the linear extrapolation to the weld toe from stresses at positions a and b, cf. Fig. 1. These positions are defined in the same guideline as a function of the brace radius and thickness. Only maximum principal stress S_1 is used for the sake of simplicity. S_1 is defined as the maximum component of the stress tensor when the reference is rotated such that the shear components become zero. It is found that this approximation is accurate enough, being the differences between the principal stress and the stress normal to the weld negligible at the crown position [9,10].

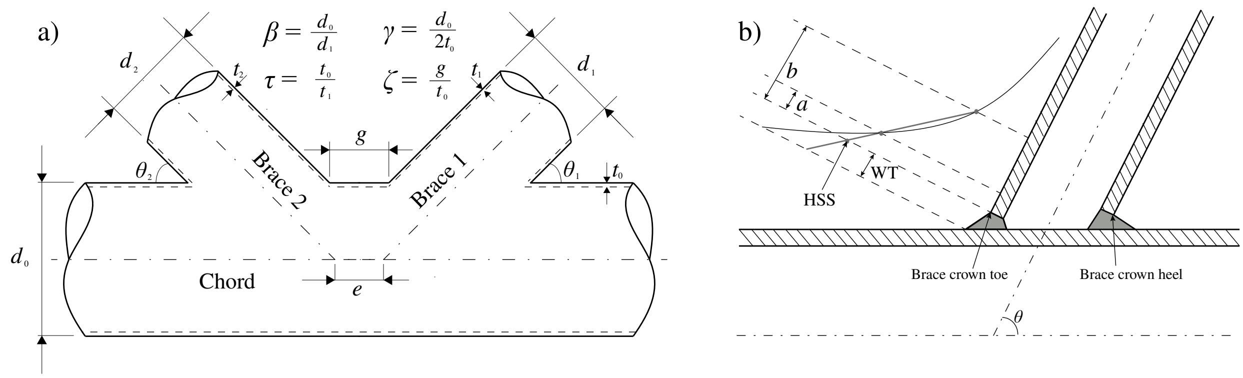

Fig. 1. (a) Sketch of the modelled K-joint and the geometrical parameters; (b) Illustration of the hot-spot stress method: The HSS is computed as the linear extrapolation to the weld toe (WT) of the structural stress evaluated at read-out points *a* and *b*.

The hot-spot stress philosophy neglects the non-linear stress peak due to the weld itself, i.e. only the structural stress behaviour is regarded. The hot-spot method avoids the stress singularity at the intersection by extrapolating the structural stress from a region out of the influence of the sharp intersection. This justifies the use of linear elastic material behaviour. If the extrapolation region is well defined, it is then acceptable to use a linear extrapolation in order to find the hot-spot stress [11]. The weld geometry is not modelled in the FEA carried out in the present work. The brace side of the weld toe is set to a distance $t_0/2 + t_1$ from the brace-chord intersection in all simulations for simplicity.

2.1. FEM model description

The numerical model is implemented in the commercial software ANSYS©. Standard steel with linear elastic behaviour is used in the present study to characterise all the tubular members. A density $\rho_s = 7850$ kg/m^3, a Young modulus $E_s = 2.10 \cdot 10^{11}$ MPa and a Poisson ratio $\nu_s = 0.3$ are used. Moreover, it is assumed that dynamic effects can be neglected for the fatigue response of the tubular joint, which can therefore be represented by the quasi-static response. Under the stated hypothesis SCF is independent of the external force value for a given load case and a single value suffices for the current work.

The modelling of the boundary conditions has a great influence on the SCF. The use of several boundary conditions has been discussed in the literature [9], e.g. clamped or hinge ends of braces or chord. In this study, boundary conditions are simplified to simple supports at the chord ends (pinned-pinned), as illustrated in Fig. 3. The chord length L_0 is chosen in such a way that the stress field at the joint does not change significantly when extending it. As it can be seen in Figure 2, the influence of the chord length becomes negligible for $L/d_0 > 3$ for the case investigated. Since this study has not been performed extensively by covering more cases and the computational repercussion of increasing the chord length is not very relevant, a ratio of $L/d_0 = 5$ is taken for all simulations. Only this load configuration is used in this investigation for simplicity. It is assumed that the load case does not have a great impact in the outcome of this investigation. Thus, only the case of having balanced axial loads is considered for simplicity. The loads are applied at the ends of the braces as a multi-point constraint.

DNV-GL [1] recommends the use of 8-node shell elements. However, 4-node elements are also acceptable if mesh refinement is implemented. Two element types are used within this work in order to study the influence of 4-node vs 8-node elements. The employed element types are: (ET1) Shell43: defined by 4 nodes (one at each corner), 6 DOF at each node, linear deformation at both in-plane directions and mixed interpolation of tensorial components in the out-of-plane direction; (ET2) Shell93: defined by 8 nodes (one at each corner and mid-side of the element edges), 6 DOF at each node, quadratic deformation at both in-plane directions and linear out-of-plane distribution in the out-of-plane through thickness direction. Further information about the element properties can be found in [12].

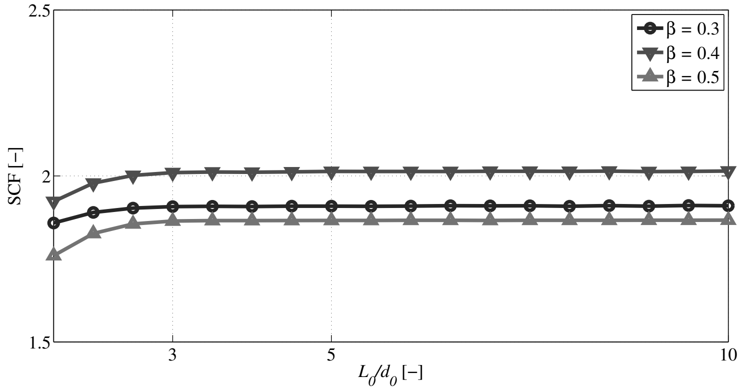

Fig. 2. Influence of extending the chord length in the computation of SCF. The following non-dimensional parameters are used to produce the data: τ = 0.5, γ = 10, θ = 45, ζ = 16.

2.2. Parametric investigation

The geometry is defined parametrically through non-dimensional joint parameters in Fig. 1.(a). A parametric investigation is carried out by varying systematically γ, τ, β and θ within ranges in Eq. (1). The braces are kept identical in all models built, i.e. $\tau_1 = \tau_2, \beta_1 = \beta_2, \theta_1 = \theta_2$ and $\zeta_1 = \zeta_2$. Subscripts are not included from this point on for simplicity. A small eccentricity is sometimes set in order to avoid overlapping of the braces. The validity ranges of the non-dimensional parameters are given for typical dimensioning due to extreme statics, dynamics, global and local stability, global fatigue analysis and weldability, according to DNV-GL [1].

$$\begin{array}{ll} 0.2 & \leq \beta \leq 1.0 \\ 0.2 & \leq \tau \leq 1.0 \\ 8 & \leq \gamma \leq 32 \\ 20^\circ & \leq \theta \leq 90^\circ \end{array} \tag{1}$$

3. Influence of the regularity of the mesh

The aim of this study is to compare efficiency and reliability of automatically generated meshes. Depending on the stress field and area where results are to be obtained, a different mesh density would be optimal. The optimum mesh is the one which gives results with the desired accuracy for the minimum computational time. Far from the joint influence, the stress field coincides with the nominal stress and therefore, a coarse meshing suffices to provide an accurate result. As a general rule, an automatically generated mesh is not optimal since the mesh density is constant along the members. Moreover, regularity of the elements within the joint influence is not controlled. Therefore, greater refinement has to be used. Nevertheless, the computational cost can be compensated in many cases with the time saved in the mesh generation phase.

Two methods of mesh generation are used in this study: full automatic generation and semi-automatic generation with parametric partitioning of the geometry. The same element type is used for both meshes in order to compare the results, i.e. SHELL43. Thus, results should converge to the same solution.

When using the ANSYS© built in algorithms of mesh generation the following procedure is applied. The mesh starts to be generated individually at each cylinder, whose ends are divided into a certain number of elements. The mesh is generated so that a continuous layout is found at the intersections. Due to that, element distortion is generally more present close to the weld positions, where results are to be extracted. An overview of this mesh layout is illustrated in Fig. 3. It can be seen that the regularity of the mesh around the brace-chord intersection is quite random. Semi-automatic mesh generation tries to avoid the latter by setting a parametric layout guided by contours that follow the weld shape within the joint influence.

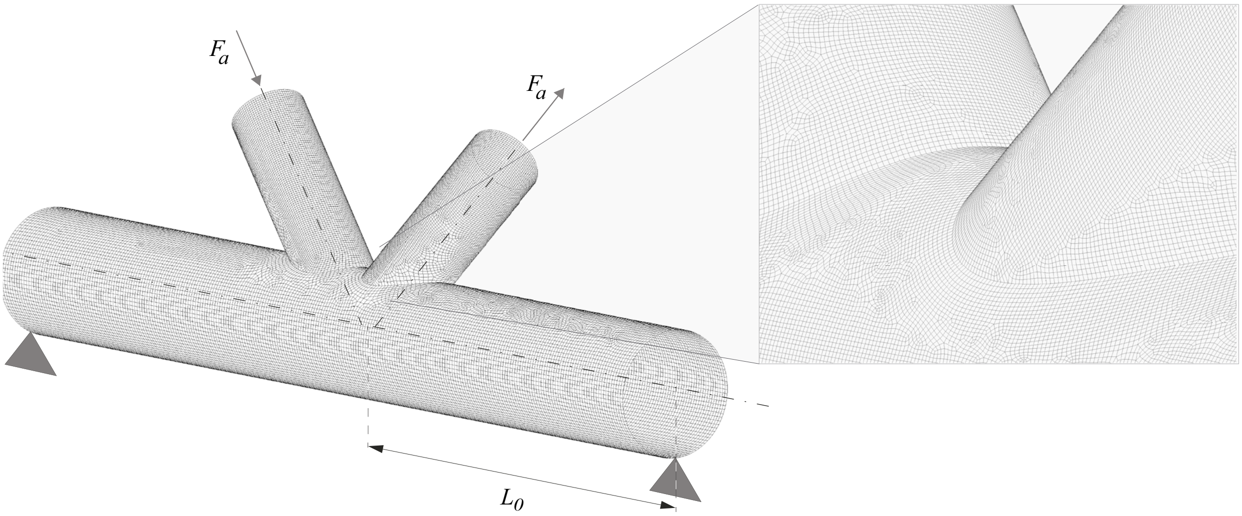

Fig. 3. Overview of the FEM model with automatically generated mesh.

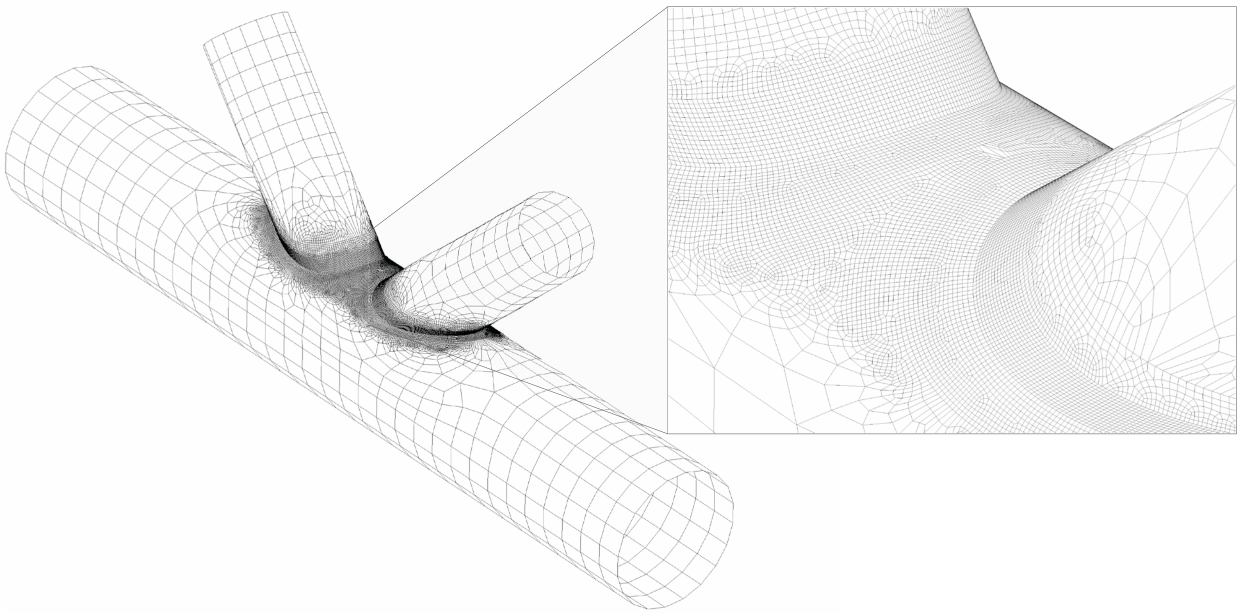

Fig. 4. Overview of the FEM model with semi-automatic mesh.

In order to obtain quadrilateral elements close to the welds, a simple generation algorithm is implemented. The braces geometries are partitioned by intersecting them with cylinders similar to the chord and with a varying offset from the chord axis. The chord geometry is partitioned with cylinders that are dilations of the braces. Quadrilateral elements are easily created between the chord-brace intersection and these lines. This type of mesh layout is shown in Fig. 4.

Both cases are compared by solving four different geometry situations for several mesh densities. The geometries are defined by $\beta = 0.6$, $\gamma = 30$, $\theta = 45°$, $\zeta = 12$ and three values of τ, i.e. 0.3, 0.5 and 0.8. Solutions are presented in Fig. 5.

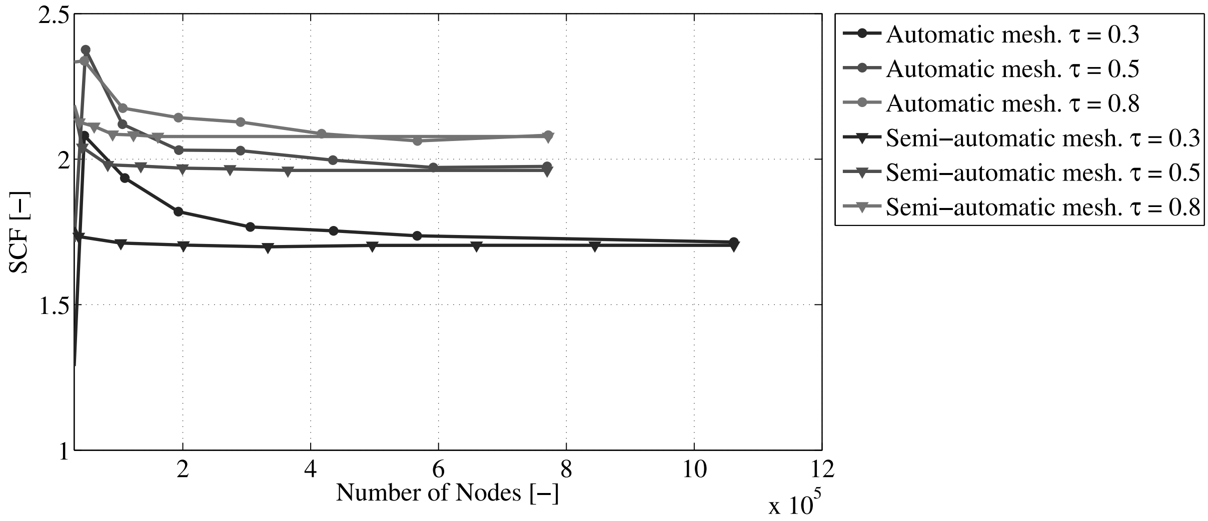

Fig. 5. Influence of mesh regularity. $\beta = 0.6$, $\gamma = 30$, $\theta = 45°$, $\zeta = 12$. 63 FEM simulations are used to produce the data in this plot.

The convergence of the solution to a constant value for increasing number of nodes is clear for the semi-automatic mesh models. This can be appreciated in Fig. 7, where little improvement is found for element size $A_{El} > t_1 \times t_1$. However, this assertion is not valid for the automatically generated mesh models. An asymptotic tendency is not obtained for all cases until a great refinement is set. Therefore, if the solution was not known a priori or the semi-automatic mesh model was not built and used as a bench mark, some cases would require further refinement to make sure that the solution obtained using around 1,000,000 nodes is accurate enough. An example of that can be seen in Fig. 5 for the case of $\tau = 0.3$.

Solutions between both kind of models match for increasing mesh density. This grants the irregular mesh model reliability for a mesh which is dense enough. However, the required element size is smaller than the one recommended in guidelines if this philosophy of mesh generation is used. The hot-spot method is proved to be quite robust in terms of mesh dependency. In general, the automatic meshing demands five times more computational time than the semi-automatic meshing for an accuracy of 1 %.

4. Influence of the element type

In order to study the influence of the element type in the computation of SCF, the same model is solved for both SHELL43 and SHELL93. The geometry of the model is characterized by the following dimensionless parameters: $\beta = 0.6$, $\tau = 0.8$, $\gamma = 30$, $\theta = 45°$, $\zeta = 12$. SCF is computed at the brace 1 toe position for varying element size in the range from $2t_1 \times 2t_1$ to $2t_1/7 \times 2t_1/7$. The properties of the FEM models and results are collected in Table 1. The last column shows the error of the SCF computed with respect to the solution for the smallest element size presented, taken as the benchmark value.

The results for both element types do not converge on the same solution. A difference of 2% exists for some cases. As expected, convergence of the results is much faster for the 8-node element, whose error for the biggest element size is already less than 2.5%. Furthermore, the required computational time of the simulations is compared, cf. Fig. 6.(a). Additional FEM simulations are carried out for β equal to 0.6 and 0.8 in order to have a broader view. It can be drawn that the computational time grows linearly with respect to the number of elements for the 4-node element and quadratically for the 8-node case.

Around 60-70% of the computational time belongs to solving the model; the remaining time is linked to building the model, which mainly consists of mesh generation. Assessing which element type is better to be used in terms of efficiency depends on the accuracy that is asked of the model. This is illustrated in Fig. 6.(b). An error of less than 1% is obtained for all the three β cases for the SHELL93 for an element size of $t_1 \times t_1$. This corresponds to around

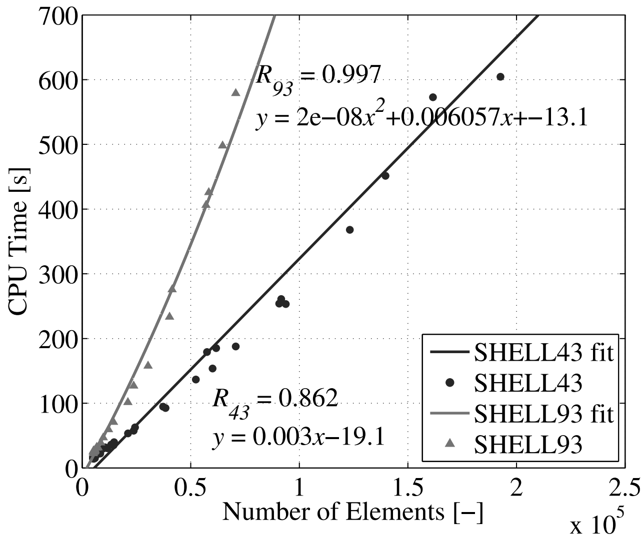

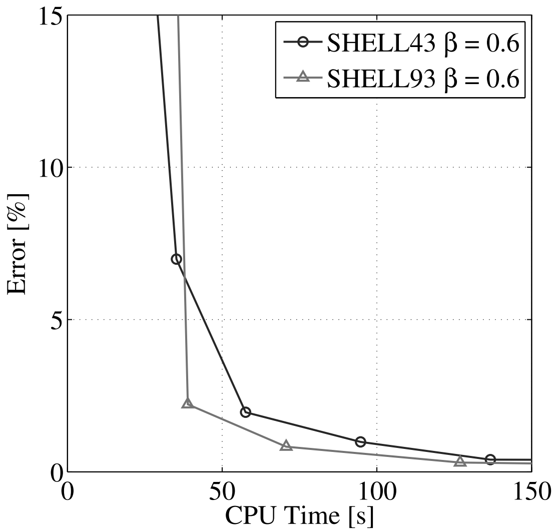

Fig. 6. Comparison of the 4-node elements versus 8-node elements in terms of accuracy and efficiency. The following parameters are used in both figures: $\tau = 0.8$, $\gamma = 30$, $\theta = 45°$, $\zeta = 12$. (a) Computational time versus number of elements using 66 FEM simulations and three different β values, i.e. 0.4, 0.6 and 0.8. (b) Error versus computational time using 10 FEM simulations and unique $\beta = 0.4$.

60 s. Same precision requires approximately 100 s for the SHELL43. If higher accuracy was asked of the model, the computational time of the 8-node element would start to rapidly increase and the 4-node element could be a more efficient solution. However, it would be unrealistic to ask for an accuracy higher than the 2% difference between the models.

Table 1. Comparison of the results of FEM simulations for the element types SHELL43 and SHELL93 using the following non-dimensional parameters: $\beta = 0.4$, $\tau = 0.8$, $\gamma = 30$, $\theta = 45°$, $\zeta = 12$.

Elem. size	Element Type	Number of elements	Number of nodes	Simulation time [s]	SCF [-]	Error [%]
$2t_1 \times 2t_1$	SHELL43	8,315	8,308	22	3.90	24.06
$2t_1 \times 2t_1$	SHELL93	85,39	25,603	39	3.17	2.22
$t_1 \times t_1$	SHELL43	14,478	14,410	35	3.36	6.98
$t_1 \times t_1$	SHELL93	14,455	43,221	71	3.12	0.82
$t_1/2 \times t_1/2$	SHELL43	37,286	37,102	95	3.17	0.98
$t_1/2 \times t_1/2$	SHELL93	41,428	123,906	276	3.10	0.11
$t_1/3 \times t_1/3$	SHELL43	70,723	70,410	188	3.16	0.40
$t_1/3 \times t_1/3$	SHELL93	70,696	211,450	579	3.14	1.43
$2t_1/7 \times 2t_1/7$	SHELL43	91,658	91,290	261	3.14	0.00
$2t_1/7 \times 2t_1/7$	SHELL93	91,560	273,926	718	3.10	0.00

5. Influence of the element size

In order to study the mesh density influence, the semi-automatic FEM model is used. The brace part of the joint influenced area which is meshed with regular quadrilateral elements, is extended to four times the brace thickness. Within this area the mesh density is controlled by a parameter here denoted refinement factor R_f, cf. Eq. 2. A parametric study for several geometry situations concerning solving 130 FEM models is carried out. Solutions are presented in Fig. 7.

$$A_{El} = t_1/R_f \times t_1/R_f \tag{2}$$

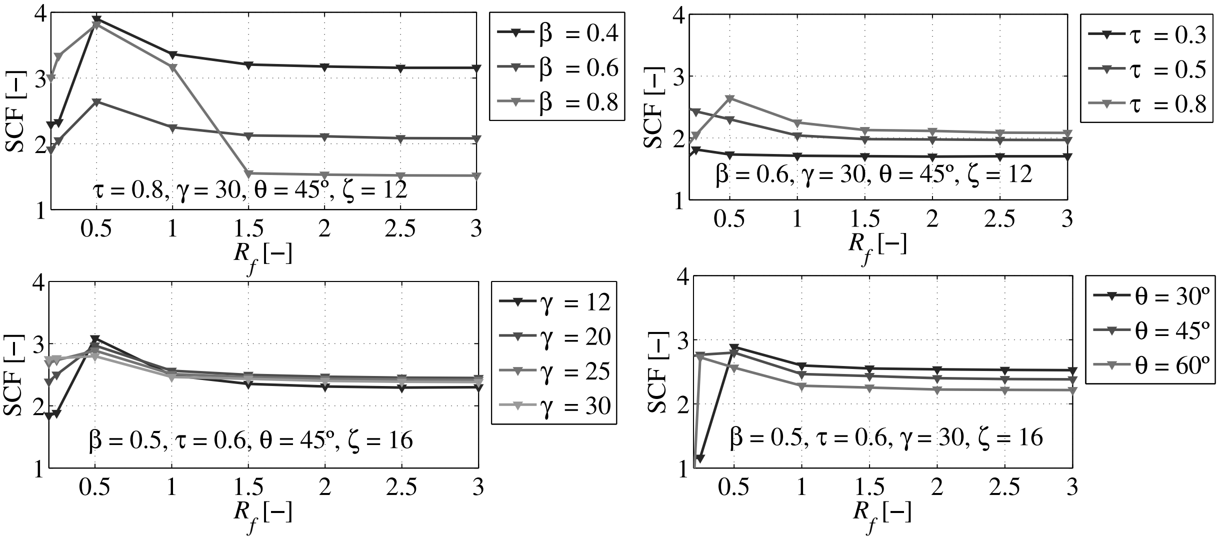

Fig. 7. Mesh density parametric study carried out using 130 FEM simulations. SCF is computed for varying refinement factor R_f and several geometry situations.

Guidelines recommend the use of an element size from $t_1 \times t_1$ up to $2t_1 \times 2t_1$, i.e. $R_f = 1$ and $R_f = 1/2$, respectively. Generally speaking, it is drawn that an element size of $t_1 \times t_1$ is appropriate for the computation of the SCF. However, some cases show large errors for this element size. An example of the latter can be seen for the situation defined by $\tau = 0.8, \beta = 0.8, \gamma = 30, \theta = 45°, \zeta = 12$. It can also be inferred that an element size of $2t_1 \times 2t_1$ tends to greatly over-predict the SCF and therefore it is not appropriate when using 4-node elements. Nevertheless, it is concluded that guidelines regarding element size are too generic and do not apply to all situations. Hence, it is recommended according to the presented results, to always perform a parametric study in order to ensure that the solution is accurate enough.

6. Conclusions

A parametric study to investigate the influence of meshing for the computation of SCF for the hot-spot method was carried out. Several FEM models are built to investigate the effect of mesh density, regularity of the elements and element type. The results are evaluated in terms of reliability and computational time.

Generally speaking, automatically generated meshes do not provide a good balance between accuracy and computational time. A great mesh refinement is needed in order to provide a trustworthy solution. In order to investigate the influence of mesh regularity, two mesh schemes were defined; semi-automatic meshing, which provides regular elements in the area of influence of the joint and automatic meshing, which provides elements with poor shape ratios. The solutions between the semi-automatic models and the automatically generated models match when the number of nodes is increased sufficiently. Thus, the use of automatically generated meshes can be justified at certain cases, since they do not require time to be spent in the manual definition of patterns to create a regular mesh.

It is found for the studied case that 8-node elements are more efficient than 4-node elements for the accuracy required in the hot-spot method. The SCF obtained by using both element types do not match, i.e. a difference of around 2% exists.

The influence of the mesh refinement at the joint influenced area was investigated. For most of the tested geometry situations, the most efficient element size is $t_1 \times t_1$. However, this is not a general rule. Using a smaller element size could yield underconservative solutions. Thus, a mesh parametric studied should always be performed.

Future work may follow regarding fatigue assessment of tubular joints of jacket structures for OWT. Three possible topics to be investigated are here presented. (1) Investigation of the accuracy of modelling multi-planar KK-joints as planar K-joints. (2) Comparison of the SCF results obtained by using shell and solid elements, assessing when it is preferable to use each element type. (3) Comparison of the SCF results obtained by following the hot-spot method and the notch stress concept.

Acknowledgements

The present study has been done at the Department of Civil and Environmental Engineering of the Norwegian University of Science and Technology. The authors would like to thank Dr.-Ing. Marc Voßbeck from Ramboll for the original idea here developed.

References

[1] Fatigue Design of Offshore Steel Structures. DNVGL-RP-C203; Oslo, Norway: DNV GL AS; 2016.
[2] Recommendations for Fatigue Design of Welded Joints and Components. IIW-2259-15; IIW; Wilhelmshaven, Germany: Springer; 2016.
[3] Efthymiou, M.. Development of SCF Formulae and Generalised Influence Functions for use in Fatigue Analysis. OTJ 88 1988;.
[4] Stress Concentration Factors for Simple Tubular Joints. Assessment of Existing and Development of New Parametric Formulae. No. 353 in OTH reports; Wimpey Offshore Lloyds Register of Shipping; London, UK: Health and Safety Executive; 1997.
[5] P. Thibaux, S.C.. Computation of Stress Concentration Factors for Tubular Joints. Proc ASME 2013 32nd International Conference on Ocean, Offshore and Arctic Engineering 2013;.
[6] S. Yong-Bo D. Zhi-Fu, L.S.T.. Prediction of hot spot stress distribution for tubular K-joints under basic loadings. Journal of Constructional Steel Research 2009;65:2011–2026.
[7] B.H. Hammerstad S. Schafhirt, M.M.. On Fatigue Damage Assessment for Offshore Support Structures with Tubular Joints. Energy Procedia 2016;94:339–346. 13th Deep Sea Offshore Wind R&D Conference, EERA DeepWind 2016.
[8] O. Doerk W. Fricke, C.W.. Comparison of Different Calculation Methods for Structural Stresses at Welded Joints. International Journal of Fatigue 2003;25:359–69.
[9] Romeijn, A.. Stress and Strain Concentration Factors of Welded Multiplanar Tubular Joints. PhD dissertation; Delft University of Technology; Civil Engineering Department; 1994.
[10] S. A. Karamanos A. Romeijn, J.W.. Stress Concentrations in Tubular Gap K-joints: Mechanics and Fatigue Design. Engineering Structures 2000;22(7):4–14.
[11] Radaj, D.. Design and analysis of fatigue resistant welded structures. Abington Publishing; 1990. Edition: Cambridge.
[12] ANSYS Mechanical APDL Users Guide; silver ed. Ansys, Inc.; Canonsburg, Pennsylvania, USA; 2013.